# Delocalization of ultracold atoms in a disordered potential due to light scattering

Boris Nowak,[1,2] Jami J. Kinnunen,[3] Murray J. Holland,[4] and Peter Schlagheck[5]

[1]*Institut für Theoretische Physik, Ruprecht-Karls-Universität Heidelberg, Philosophenweg 16, 69120 Heidelberg, Germany*

[2]*ExtreMe Matter Institute (EMMI), GSI Helmholtzzentrum für Schwerionenforschung GmbH, Planckstraße 1, 64291 Darmstadt, Germany*

[3]*Department of Applied Physics, Aalto University School of Science, Post Office Box 15100, FI-00076 Aalto, Finland*

[4]*JILA, NIST, and Department of Physics, University of Colorado, Boulder, Colorado 80309-0440, USA*

[5]*Département de Physique, Université de Liège, allée du 6 Août 17, 4000 Liège, Belgium*

(Received 22 June 2012; published 9 October 2012)

We numerically study the expansion dynamics of ultracold atoms in a one-dimensional disordered potential in the presence of a weak position measurement of the atoms. We specifically consider this position measurement to be realized by a combination of an external laser and a periodic array of optical microcavities along a waveguide. The position information is acquired through the scattering of a near-resonant laser photon into a specific eigenmode of one of the cavities. The time evolution of the atomic density in the presence of this light-scattering mechanism is described within a Lindblad master equation approach, which is numerically implemented using the Monte Carlo wave function technique. We find that an arbitrarily weak rate of photon emission leads to a breakdown of Anderson localization of the atoms.

DOI: 10.1103/PhysRevA.86.043610 PACS number(s): 03.75.−b, 42.50.Ct, 67.85.−d, 03.65.Yz

## I. INTRODUCTION

The realization of potentials with controlled disorder for ultracold atoms has recently led to the observation of Anderson localization with Bose-Einstein condensates [1,2]. In those experiments, atomic Bose-Einstein condensates, prepared in a harmonic trap, were released into one-dimensional optical waveguides, which were superimposed with disordered potentials realized with speckle fields [1,3,4] as well as with bichromatic optical lattices [2,5]. Absorption images of the atomic cloud after the expansion process within the waveguide clearly revealed an exponential decrease of the average atomic density with the distance from the center of the former trap, which is the characteristic signature of Anderson localization [6]. While interaction effects were not the focus of those pioneering experiments, more recent studies specifically explored the interplay of atom-atom interaction and localization in disordered potentials (e.g., Refs. [7,8]). Current research directions include the exploration of Anderson localization with ultracold atoms in three spatial dimensions [9,10], with the particular aim of studying the Anderson metal-insulator transition [11].

Clearly, a key condition for the observability of Anderson localization with ultracold atomic gases is the overall coherence of the atomic cloud. Any mechanism of decoherence would compromise the phenomenon of destructive wave interference that lies at the heart of Anderson localization [6] and thereby give rise to delocalization. This also concerns any *in situ* monitoring of the evolution of the atomic cloud during its expansion, by intermediate measurements of the positions of atoms. Evidently, the strong refocusing of the atomic wave function that results from a precise position measurement would destroy the coherence of the atom, enhance its kinetic energy, and eventually (when performed several times) let the atom behave as a classical particle.

The situation is less obvious for "weak" measurement processes, in which the position of the atom is determined with a large spatial uncertainty that is of the order of the expected localization length within the disordered potential. Such weak measurements might still preserve coherence to a certain extent, while, at the same time, providing some rough *in situ* information on the position of the atom. For this purpose, one could, for example, conceive of a periodic array of optical microcavities placed around the waveguide in which the atoms propagate, as depicted in Fig. 1. A near-resonant laser beam which irradiates this configuration can be used to transfer the atoms to an electronically excited state, from which they can relax to the ground state by a spontaneous emission of a photon into one of the cavities. Such emitted photons could in turn be measured by photodetectors placed behind the cavities [12]. The whole configuration possibly could be fabricated on "atom chips" [13], in which case the disordered potential could arise from imperfections in the current-carrying wires that generate the magnetic waveguide potential of the atoms [14,15]. However, our results below are more general and we expect to see the same effects on the localization in the presence of any mechanism of similar position measurement.

The aim of this study is to investigate to which extent this approximate realization of a "Heisenberg microscope" gives rise to delocalization of an atom in a one-dimensional disordered potential. For the sake of simplicity, we restrict our consideration to the propagation of one single atom and thereby discard collective processes arising within Bose-Einstein condensates due to atom-atom interactions or superradiance. Moreover, we assume that the atom will emit photons into one single mode of the cavities only. Such an emission will then give rise to a recoil that is mainly perpendicular to the direction of propagation of the atom and does therefore not dramatically enhance its longitudinal kinetic energy. We neglect effects of transverse excitations within the waveguide due to this recoil and assume that neither the effective waveguide confinement nor the disordered potential are affected by temporary populations of the excited electronic state of the atom.

The dynamics of the atom is modeled via a one-dimensional master equation for its density matrix $\hat{\rho}(t)$, which can be unraveled using the Monte Carlo wave function technique

 

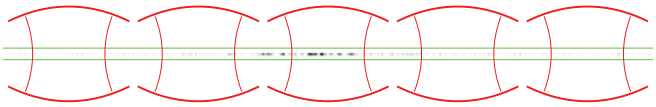

FIG. 1. (Color online) Sketch of the configuration under consideration. An atom, which is initially localized within a harmonic trap at the center, is expanding within a one-dimensional waveguide (indicated by the green [light gray] horizontal lines) to which a disordered potential is superimposed. A periodic array of optical microcavities (symbolized by the red [dark gray] arcs) is used to measure the position of the atom, on a length scale that is comparable to its localization length (indicated by the shadow plot in the waveguide, which shows the density of a localized state). For this purpose, the waveguide is considered to be irradiated by a near-resonant laser beam, which may induce spontaneous emissions of photons into one of the cavities, possibly to be measured by photodetectors. The sketch is to scale with the parameters considered in this study, as far as the horizontal length scales are concerned.

[16,17]. This master equation accounts both for the coherent motion within the disordered potential and the incoherent scattering of photons [18]. Similar tools have been used to study dynamics of a (disorder-free) Bose-Einstein condensate in the presence of a continuous position measurement induced by an off-resonant laser beam [19]. In Sec. II, we first describe the expansion and localization dynamics of a single atom in a one-dimensional disordered potential in the absence of any decoherence mechanism. In Sec. III, we outline the Monte Carlo wave function approach that is used to integrate the master equation for the special case of an atom that propagates in a homogeneous, disorder-free waveguide. Decoherence and disorder are finally put together in Sec. IV, in which we discuss the expansion of an atomic wave packet in the presence of disorder and spontaneous emission. We show that even very rare position measurements of the atom give rise, on average, to a gradual delocalization of the wave packet, and we provide numerical evidence for superballistic expansion in the presence of strong emission rates.

## II. WAVE PACKET EXPANSION IN DISORDER

In this section, the expansion of an initially trapped wave packet in a weak one-dimensional disordered potential is discussed. For the sake of simplicity, we model the disorder by a Gaussian correlated random potential $V(x)$ defined along the $x$ axis, with the properties $\overline{V(x)} = 0$ and

$$\overline{V(x)V(x')} = U^2 \exp[-(x-x')^2/(2\sigma^2)] \tag{1}$$

for the mean spatial correlation function. Here, $U$ characterizes the typical size of the fluctuations of the potential, and the correlation length $\sigma$ controls the average width of fluctuations.

In Fig. 2 we show the time evolution of the disorder-averaged spatial density of wave packets propagating in such disorder configurations. These wave packets are initially prepared in the ground state of a harmonic trap with the oscillator length $a_0 = \sqrt{\hbar/m\omega}$. After the trapping potential is switched off, the wave packet expands within the disordered potential until it approaches, on average, a stationary profile. The convergence to the average density distribution happens faster at the center than in the wings. This is a consequence of

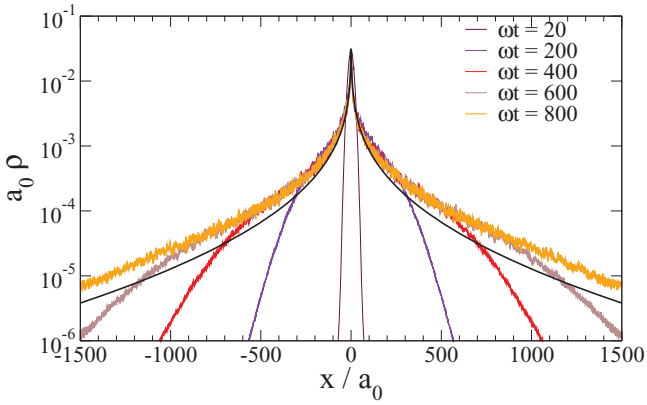


FIG. 2. (Color online) Time evolution of the expansion process of a Gaussian wave function, averaged over 100 disorder realizations, for the strength $U = 0.1\,\hbar\omega$ and the correlation length $\sigma = 0.2\,a_0$ of the disordered potential (the mean initial kinetic energy of the wave function is $E = 0.25\,\hbar\omega$, where $a_0$ and $\omega$ are the oscillator length and the frequency of the harmonic confinement potential, respectively). Shown are the disorder-averaged probability densities $\rho(x)$ for $\omega t = 20$, 200, 400, 600, and 800 (with the trap opening at $t = 0$). The solid line displays the analytical prediction (5) which is found to be in good agreement with the numerical density distribution at large distances $|x| \gg a_0$, apart from a global prefactor of the order of 2.

the quadratic growth of the localization length as a function of the wave vector, as described in Eq. (3) below.

The final density profile shown in Fig. 2 is fairly well reproduced by a theory described in Ref. [20], which is based on the assumption that the asymptotic probability distribution is an incoherent sum of individually localized plane waves with momentum $p$ (see Ref. [4] for an alternative and more elaborate theoretical approach). This consideration yields the spatial density

$$\rho_{\rm loc}(x) = \int dp \frac{\rho_0(p)}{2\xi(p)} \exp[-|x|/\xi(p)], \tag{2}$$

where $\rho_0$ denotes the momentum density of the wave packet at the initial time $t = 0$. The key ingredient for the evaluation of Eq. (2) is the localization length $\xi(p)$ that can be calculated as $\xi(p) = 2l_B(p)$, with $l_B$ being the Boltzmann mean free path [21–23]. For the Gaussian correlated random potential under consideration, we obtain

$$\xi(p) = \frac{1}{\sqrt{2\pi}} \frac{\hbar^2 p^2}{m^2 U^2 \sigma} \exp[2(p\sigma/\hbar)^2]. \tag{3}$$

In the regime of short correlation lengths $\sigma \ll \hbar/p$, we can approximate $\exp[2(p\sigma/\hbar)^2] \simeq 1$ and the localization length depends only on the effective strength $U^2\sigma$ of the disorder. Using

$$\rho_0(p) = \frac{a_0}{\sqrt{\pi}\hbar} \exp[-(a_0 p/\hbar)^2] \tag{4}$$

and introducing the characteristic localization length scale of the wave packet as $\xi_0 \equiv \xi(\hbar/a_0)$, we then obtain the prediction

$$\rho_{\rm loc}(x) = \frac{1}{2\sqrt{\xi_0|x|}} \exp(-2\sqrt{|x|/\xi_0}) \tag{5}$$

for the localized density. As shown in Fig. 2, this approximate expression is, apart from a global prefactor, in good agreement with the numerically computed mean density at the final time $t = 800/\omega$.

In the above numerical simulations, we effectively assumed that the atomic cloud is prepared in a clean harmonic trap in the absence of any disorder. At $t = 0$ the trapping potential is suddenly switched off and the disorder is ramped on at the same time. The initial state is then a perfect Gaussian wave function [see Eq. (4)] which expands within the disordered potential. In general, this procedure is not precisely in accordance with expansion experiments on Anderson localization such as Ref. [1], in which the disordered potential is already present during the formation of the Bose-Einstein condensate in the harmonic trap. The initial state of the atomic wave function in that case is given by the ground state of an effective trapping potential that consists of a harmonic confinement modulated by the disorder. A numerical comparison of these two expansion scenarios, however, displays no significant difference in the asymptotic density profile for the case of weak disordered potentials with $U \simeq 0.1\hbar\omega$ and $\sigma = 0.2\,a_0$.

A convenient numerical observable for measuring localization is the participation ratio [24] which for a wave packet with the density $\rho(x,t)$ is defined by

$$R_P(t) = \left( \int_{-\infty}^{\infty} dx [\rho(x,t)]^2 \right)^{-1}. \tag{6}$$

In practice, $R_P(t)$ represents a measure for the spatial extent of the wave packet, yielding large values for rather extended distributions $\rho(x,t)$ and going to zero for strongly peaked wave functions. It therefore exhibits a similar behavior to the spatial root mean square (rms) width $\Delta x = \sqrt{\langle x^2\rangle - \langle x\rangle^2}$ of the wave packet. However, this latter quantity is rather sensitive to the evolution of the (experimentally inaccessible) wings of the wave packet. This is shown in Fig. 3, where we display the time dependence of the disorder-averaged rms width and participation ratio. While the rms width continuously increases with time, due to the long-time dynamics in the wings of the

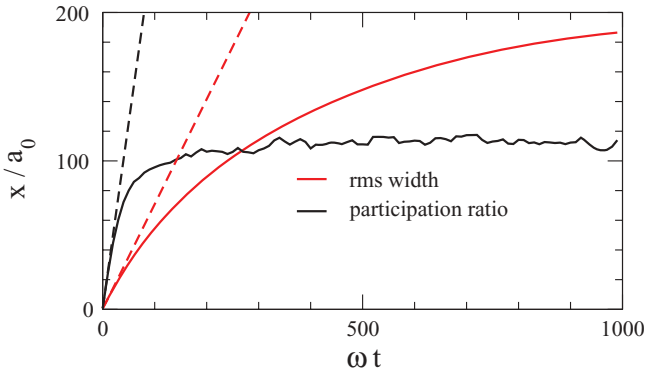


FIG. 3. (Color online) Root mean square (rms) width $\Delta x = \sqrt{\langle x^2\rangle - \langle x\rangle^2}$ (red line) and participation ratio $R_P(t)$ (black line) as a function of the evolution time $t$, showing the disorder average of the expansion and localization of a wave packet for the disorder strength $U = 0.15\hbar\omega$ and the correlation length $\sigma = 0.2\,a_0$. The dashed lines show, for comparison, the rms width and the participation ratio of a free wave packet that expands in the absence of disorder.

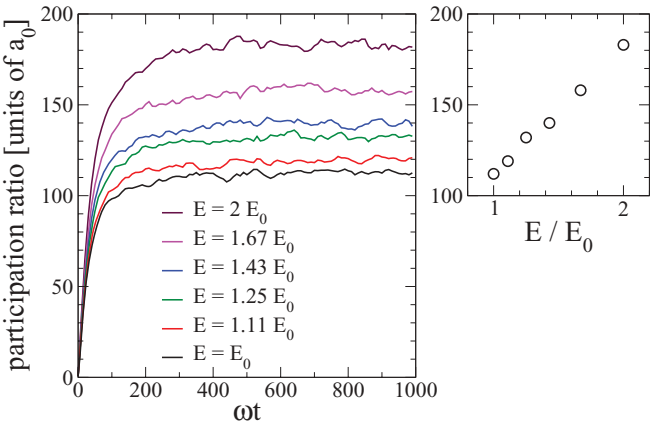


FIG. 4. (Color online) Left panel: disorder-averaged participation ratio as a function of time for different initial kinetic energies $E$, with $E_0 = 0.25\hbar\omega$. The disordered potential is characterized by the parameters $U = 0.15\hbar\omega$ and $\sigma = 0.2\,a_0$. The right panel shows the temporal average of this participation ratio within $400 < \omega t < 1000$ as a function of the energy $E$. This average defines the asymptotic localization length $L_{\rm wp}$ of the wave packet. $L_{\rm wp}$ is found to increase approximately linearly with the initial kinetic energy.

averaged density distribution (see Fig. 2), the participation ratio, which is much less sensitive to the behavior of the wings, saturates at a finite length scale. This length scale can be used in order to define an effective localization length $L_{\rm wp}$ of the wave packet.

Figure 4 shows the time evolution of the disorder-averaged participation ratio for different initial kinetic energies $E$, resulting from different confinement frequencies of the initial trapping potential. A linear increase of the participation ratio with $E$, corresponding to a linear increase of the effective localization length $L_{\rm wp}$ of the wave packet, is found for $E_0 < E < 2E_0$.

## III. MASTER EQUATION DYNAMICS

To account for spontaneous emissions of photons into the cavities, we model the dynamics of the atom via a one-dimensional master equation for its density matrix $\hat{\rho}(t)$, including coherent interactions with a disordered potential and the incoherent scattering of light [18]. This master equation is given by

$$\frac{d}{dt}\rho(t) = -\frac{i}{\hbar}[\hat{H},\hat{\rho}(t)] + \gamma_{\rm eff}\int_{-k}^{k}\frac{dq}{2k}[\hat{C}_q\hat{\rho}(t)\hat{C}_q^\dagger - \hat{\rho}(t)]. \tag{7}$$

Here, $\hat{H} = \frac{\hat{p}^2}{2m} + V(\hat{x})$ describes the Hamiltonian for a particle that propagates in the disordered potential. $\hat{C}_q = e^{-iq\hat{x}}$ is the decay or jump operator representing one spontaneous emission event, which exerts a recoil on the atom with longitudinal momentum $\hbar q$, which is assumed to be equidistributed between $-\hbar k$ and $+\hbar k$. This model considers off-resonant inelastic scattering, in which a laser couples the electronic ground state to an excited state from which spontaneous emission back to the ground state can occur. It assumes a low spontaneous decay rate $\gamma$ as compared to the detuning $\delta$ of the laser with respect to the intra-atomic transition frequency and

a low Rabi frequency $\nu$ for laser-induced transitions between the ground state and the excited state as compared to the spontaneous decay rate $\gamma$; that is, we assume $\nu \ll \gamma \ll \delta$. We then obtain $\gamma_{\rm eff} = \gamma\nu^2/(\gamma^2 + 4\delta^2)$ as the effective decay rate that enters the master equation (7) [25,26].

To solve the time evolution generated by the master equation, we employ the Monte Carlo wave function method [16,17]. Here, the evolution of the density matrix is decomposed into the nonunitary evolution of a large number $N = 100$ of wave functions. A single trajectory $|\psi\rangle_i, i = 1,\ldots,N$ evolves according to $i\hbar\partial_t|\psi\rangle_i = \hat{H}_{\rm eff}|\psi\rangle_i$ with $\hat{H}_{\rm eff} \equiv \hat{H} - i\gamma_{\rm eff}/2$, until the exponentially decaying norm $||\psi\rangle_i|^2 = e^{-\gamma_{\rm eff}t}$ equals a random number chosen between 0 and 1. At this point, a jump operator $\hat{C}_q$ acts on the Monte Carlo wave function: $|\psi(t+\delta t)\rangle_i = \hat{C}_q|\psi(t)\rangle_i$. This jump operator is, for the sake of simplicity of the analysis, determined by randomly choosing $q$ from the interval between $-k$ and $k$.

To relate this light-scattering process to the position measurement under consideration, we note that the Lindblad master equation is invariant under unitary transformations on the set of decay operators. Indeed, it was shown in Ref. [27] that the Fourier transformation $\int_{-1}^{1} du\, \exp(iuk\nu\lambda/2)\,\hat{C}_u$ with integers $\nu \in \mathbb{Z}$ allows one to switch to decay operators

$$\hat{C}_\nu = \sqrt{2}\frac{\sin\left(k\hat{x} - \frac{\nu}{2}\right)}{k\hat{x} - \frac{\nu}{2}}. \tag{8}$$

In this picture, the application of the decay operator induces a localization of the wave function within a spatial region whose extent is of the order of $k^{-1}$. Within the framework of the weak measurement configuration outlined in the introduction, we assume that these decay operators exactly correspond to the longitudinal structure of the cavity modes into which the atom may emit the photon. The spatial period of the array of cavities is then given by $\lambda = 2\pi/k$.

In Fig. 5, we show the time evolutions of the expectation value of the position $\langle x\rangle$ and its rms width $\Delta x = \sqrt{\langle x^2\rangle - \langle x\rangle^2}$ for a single quantum trajectory in free space, $V(x) = 0$. In this particular trajectory, the first spontaneous emission took place in one of the two wings of the wave packet, which is mainly constituted by plane-wave components with high momenta. The subsequent localization process projects the wave function on those high-momentum components, which gives rise to a permanent drift. The rms width, however, remains small during this evolution, which is due to the fact that the atom emits photons at a rate that is faster than the inverse dispersion time of the wave packet. The rms width would freeze for sufficiently high emission rates, which is reminiscent of the quantum Zeno effect.

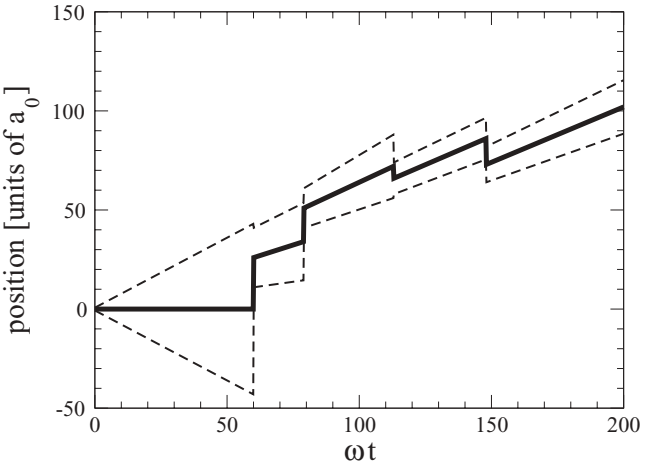


FIG. 5. Center-of-mass position $\langle x\rangle$ (solid line) for a single trajectory of an atom that is subject to light scattering with $k = 0.07/a_0$. The dashed lines indicate the root mean square (rms) width $\Delta x = \sqrt{\langle x^2\rangle - \langle x\rangle^2}$; that is, they correspond to the lines $\langle x\rangle \pm \Delta x$. Photon emissions occur at $\omega t = 60$, 79, 113, and 148.

It is of great advantage to work in a regime where $k$ is small compared to fluctuations of the density matrix in momentum space $\rho(p,p',t)$. To study the momentum density distribution, we can then approximate the integrand of Eq. (7) by its Taylor expansion to first order, as was done in Ref. [28]. Taking the integral over $k$ leads to the diffusion equation

$$\partial_t\rho(p,t) = \tfrac{1}{6}\gamma_{\rm eff}k^2\partial_p^2\rho(p,t) \tag{9}$$

for the diagonal elements of the density matrix, with the effective diffusion coefficient $D = \gamma_{\rm eff}k^2/6$. Hence, the wave packet will undergo diffusive spreading in momentum space. Noting that the variance of the momentum distribution is nothing but the kinetic energy, we obtain

$$\langle\hat{T}\rangle = {\rm Tr}\left\{\frac{\hat{p}^2}{2m}\hat{\rho}(t)\right\} = E_0 + \frac{\hbar^2k^2}{6m}\gamma_{\rm eff}t \tag{10}$$

for the growth of the mean kinetic energy of the wave packet.

## IV. DISSIPATIVE EXPANSION IN DISORDER

Having introduced the necessary tools, we now study wave packet expansion in the presence of disorder and dissipation. In Fig. 6 we plot the disorder average of the participation ratio

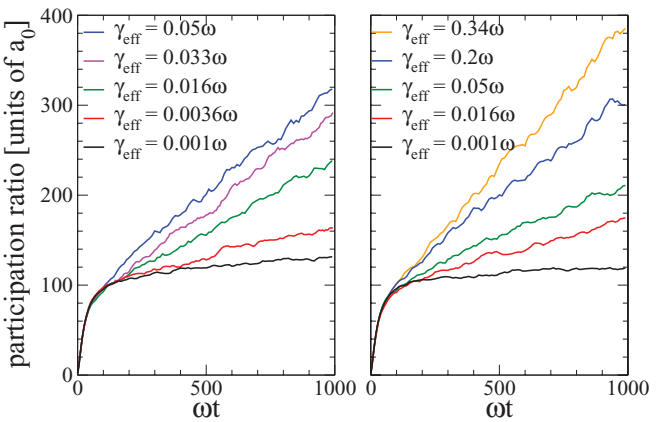


FIG. 6. (Color online) Master equation dynamics of the disorder-averaged participation ratio for different effective emission rates $\gamma_{\rm eff}$. The longitudinal momentum of the emitted photon is $k = 0.07/a_0$ in the left panel and $k = 0.035/a_0$ in the right panel. The linear growth of the participation ratio for $\omega t \gtrsim 100$ reflects the growth of the mean kinetic energy due to photon scatttering events, which is found to increase from $E = 0.25\,\hbar\omega$ at $t = 0$ to $E \simeq 0.5\,\hbar\omega$ at $\omega t = 1000$ for $k = 0.07/a_0$ and $\gamma_{\rm eff} = 0.05\omega$ (blue [top] curve in the left panel). The disordered potential is characterized by the strength $U = 0.15\,\hbar\omega$ and the correlation length $\sigma = 0.2\,a_0$.

as a function of time for different effective emission rates $\gamma_{\rm eff}$. In accordance with the sketch shown in Fig. 1, we have chosen the photon wavelength to be very long compared to the initial extension $a_0$ of the wave packet. The amount of kinetic energy given to the wave packet at each emission event is thereby reduced.

The most important observation is a delocalization of the wave packet at any emission rate. Instead of saturating to a stationary value, the participation ratio linearly increases with time after the typical time scale that is needed for developing an Anderson-localized density profile in the absence of spontaneous emission. Quantitatively, this linear growth is very different from a ballistic expansion in free space, which takes place with much faster expansion velocities (see the dashed lines in Fig. 3). It is also different from simple diffusion which one would naively expect to prevail for a quantum particle that propagates within a disordered potential in the presence of a decoherence mechanism. We attribute this difference to the fact that the spontaneous emission of a photon gives rise to a recoil of the atom and thereby increases its energy. Hence, the effective diffusion constant should also gradually increase with time.

In this context, it is interesting to note that the expansion velocity $dR_P/dt$ depends only on the product of the effective rate of emission $\gamma_{\rm eff}$ and the recoil energy $\hbar^2k^2/(2m)$. This can be seen by comparing the two blue lines in Fig. 6 (top line in the left panel and second from top in the right panel), showing expanding participation rates for $k = 0.07/a_0$ and $\gamma_{\rm eff} = 0.05\omega$ (left panel) as well as for $k = 0.035/a_0$ and $\gamma_{\rm eff} = 0.2\omega$. There appears to be no change in the behavior when we tune the rate of emissions across the scale $1/T_{\rm loc}$, with $T_{\rm loc}$ the time at which the unperturbed evolution shows localization.

It is tempting to relate the linear increase of the participation ratio with time to the combination of a linear growth of the kinetic energy due to spontaneous emission with the approximately linear scaling of the wave packet's localization length with its mean kinetic energy in the absence of spontaneous emission, as shown in Fig. 4. This reasoning essentially assumes that in between two subsequent spontaneous emission events the wave packet has enough time to approach its asymptotic stationary profile within the disordered potential (see also Ref. [29] for a similar discussion in a two-dimensional disordered potential). Extracting from Fig. 4 the approximate scaling $R_P/a_0 \sim 100E/E_0$ and using $dE/dt = \hbar^2k^2\gamma_{\rm eff}/(6m)$ for the growth rate of the energy according to Eq. (10), we obtain the prediction

$$\frac{dR_P}{dt} \simeq 100\,\frac{a_0}{E_0}\,\frac{dE}{dt} \simeq 400\,\frac{\gamma_{\rm eff}\hbar^2k^2}{6m}\,\frac{a_0}{\hbar\omega} \qquad (11)$$

for the expansion velocity $dR_P/dt$ of the average participation ratio, using $E_0 = 0.25\hbar\omega$.

Figure 7 shows, however, that this expansion velocity increases more strongly with the rate of increase of the kinetic energy than predicted by Eq. (11). As a matter of fact, $dR_P/dt$ is found to scale as a square root of $dE/dt$ in the parameter regime in which we carried out our numerical investigations. One may attribute this behavior to the fact that the above reasoning applies to an *individual* quantum trajectory in the spirit of Fig. 5. The energy of the wave packet corresponding to each individual trajectory increases

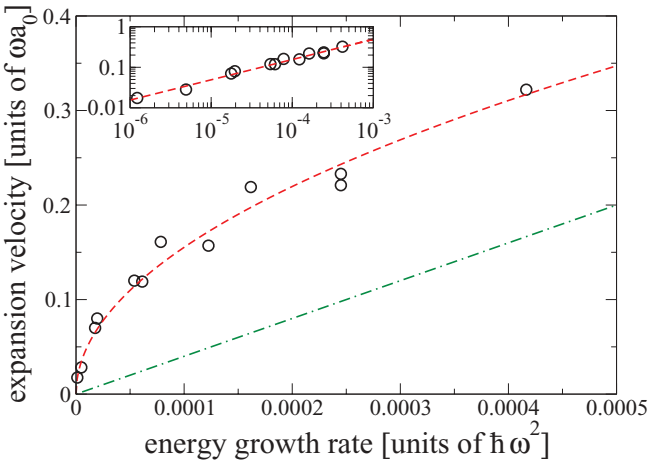


FIG. 7. (Color online) Expansion velocity $dR_P/dt$ of the disorder-averaged participation ratio as a function of the energy growth rate $dE/dt = \gamma_{\rm eff}\hbar^2k^2/(6m)$. The data are extracted from Fig. 6, as well as from other calculations using different parameters for $\gamma_{\rm eff}$ and $k$, through linear regression of the participation ratio within $100 < \omega t < 1000$. As confirmed in the log-log plot shown in the inset, $dR_P/dt$ scales as the square root of $dE/dt$: we have $dR_P/dt \simeq \alpha(dE/dt)^{1/2}a_0/\hbar^{1/2}$ with the fitted proportionality constant $\alpha \simeq 15.5$, as indicated by the dashed line. The dash-dotted straight line in the main panel represents the prediction of Eq. (11).

linearly and its participation ratio increases on average as described by Eq. (11). However, while different trajectories describe similar narrow wave packets, each wave packet will be centered around a different point in space. Thus the full (incoherent) density will be spreading faster over a larger region than a single wave packet (as is obvious from Fig. 5 for the case of disorder-free propagation). This effect is obviously not accounted for in the considerations leading to Eq. (11).

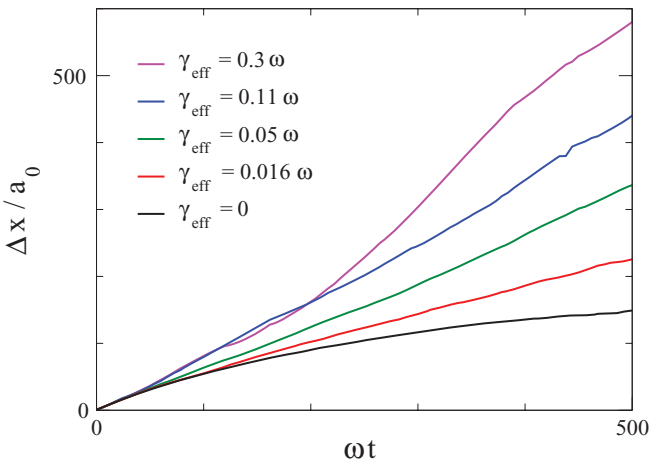


FIG. 8. (Color online) Master equation dynamics of the rms width $\Delta x$ at strong recoil $k = 0.35/a_0$ for different effective emission rates $\gamma_{\rm eff}$ and different realizations of the disordered potential which is characterized by the parameters $U = 0.15\hbar\omega$ and $\sigma = 0.2\,a_0$. We note that the growth of $\Delta x$ for $\gamma_{\rm eff} = 0.05\ \omega$ (green [middle] curve) coincides with the one of a free ballistic expansion, while superballistic expansion is encountered for larger emission rates.

Let us finally investigate the regime of strong dissipation for which it is expected that the expansion becomes independent of the disordered potential. In Fig. 8 the momentum recoil is set to $k = 0.35/a_0$, leading to a regime in which the rms width turns out to serve as an accurate measure of expansion. In this case, the recoil induced by the emitted photons may drive the system beyond the free ballistic growth into a superballistic regime, which is the valid limit of a driven expansion in free space [28]. As can be seen in Fig. 8, this superballistic regime sets in beyond $\gamma_{\rm eff} = 0.05\,\omega$ for $k = 0.35/a_0$.

## V. CONCLUSION

In summary, we have shown that even a very weak rate of photon scattering gives rise to a breakdown of Anderson localization of an atom that propagates in a one-dimensional disordered potential. This observation is consistent with similar findings obtained for a one-dimensional lattice model, in which one of the lattice sites is considered to be coupled to a measurement device [30]. The breakdown of Anderson localization is most conveniently quantified in terms of the disorder-averaged participation ratio of the atomic density, which represents a measure for the spatial width of the atomic wave packet. While this participation ratio saturates, within a characteristic time scale, to a finite value in the case of a perfectly coherent expansion process within the disordered potential, it is found to linearly grow with time beyond that time scale in the presence of spontaneous photon scattering.

This growth behavior imposes strong limits for the observability of Anderson localization in the presence of a weak position measurement of the atom. However, an experimental realization of a "Heisenberg microscope" for cold atoms according to the scheme displayed in Fig. 1 might nevertheless be of interest as it allows one to study in more detail the interplay of disorder and measurement-induced delocalization phenomena not only for a single atom but also (and this more naturally) for a Bose-Einstein condensate in which the atoms interact with each other. For this purpose, an integrated setup on atom chips appears as the most convenient realization of such a Heisenberg microscope for atomic gases.

Finally, we expect similar findings in the presence of other mechanisms that can behave as a position measurement of the propagating atom. Such mechanisms include noise on the lattice beams as well as collisions with background gas atoms, to mention two examples. Undesired effects of this type are therefore also expected to induce a delocalization of the atom in the disorder potential.

## ACKNOWLEDGMENTS

The authors thank K. Hornberger, C. A. Müller, and B. M. Peden for useful discussions. M.H. acknowledges support from the National Science Foundation.

[1] J. Billy, V. Josse, Z. Zuo, A. Bernard, B. Hambrecht, P. Lugan, D. Clément, L. Sanchez-Palencia, P. Bouyer, and A. Aspect, Nature (London) **453**, 891 (2008).
[2] G. Roati, C. D'Errico, L. Fallani, M. Fattori, M. Fort, C. Zaccanti, G. Modugno, M. Modugno, and M. Inguscio, Nature (London) **453**, 895 (2008).
[3] J. E. Lye, L. Fallani, M. Modugno, D. S. Wiersma, C. Fort, and M. Inguscio, Phys. Rev. Lett. **95**, 070401 (2005).
[4] L. Sanchez-Palencia, D. Clément, P. Lugan, P. Bouyer, G. V. Shlyapnikov, and A. Aspect, Phys. Rev. Lett. **98**, 210401 (2007).
[5] B. Damski, J. Zakrzewski, L. Santos, P. Zoller, and M. Lewenstein, Phys. Rev. Lett. **91**, 080403 (2003).
[6] P. W. Anderson, Phys. Rev. **109**, 1492 (1958).
[7] B. Deissler, M. Zaccanti, G. Roati, C. D'Errico, M. Fattori, M. Modugno, G. Modugno, and M. Inguscio, Nat. Phys. **6**, 354 (2010).
[8] E. Lucioni, B. Deissler, L. Tanzi, G. Roati, M. Zaccanti, M. Modugno, M. Larcher, F. Dalfovo, M. Inguscio, and G. Modugno, Phys. Rev. Lett. **106**, 230403 (2011).
[9] S. S. Kondov, W. R. McGehee, J. J. Zirbel, and B. DeMarco, Science **334**, 66 (2011).
[10] F. Jendrzejewski, A. Bernard, K. Müller, P. Cheinet, V. Josse, M. Piraud, L. Pezzé, L. Sanchez-Palencia, A. Aspect, and P. Bouyer, Nat. Phys. **8**, 398 (2012).
[11] J. Chabé, G. Lemarié, B. Grémaud, D. Delande, P. Szriftgiser, and J. C. Garreau, Phys. Rev. Lett. **101**, 255702 (2008).
[12] The presence of such photodetectors in addition to the cavities is not relevant for the dissipative dynamics of the atoms studied in this paper.
[13] J. Fortágh and C. Zimmermann, Rev. Mod. Phys. **79**, 235 (2007).
[14] J. Estève, C. Aussibal, T. Schumm, C. Figl, D. Mailly, I. Bouchoule, C. I. Westbrook, and A. Aspect, Phys. Rev. A **70**, 043629 (2004).
[15] T. Paul, P. Leboeuf, N. Pavloff, K. Richter, and P. Schlagheck, Phys. Rev. A **72**, 063621 (2005).
[16] C. W. Gardiner, A. S. Parkins, and P. Zoller, Phys. Rev. A **46**, 4363 (1992).
[17] K. Mølmer, Y. Castin, and J. Dalibard, J. Opt. Soc. Am. B **10**, 524 (1992).
[18] M. Schlosshauer, *Decoherence and the Quantum-to-Classical Transition* (Springer, Berlin, 2007).
[19] D. A. R. Dalvit, J. Dziarmaga, and R. Onofrio, Phys. Rev. A **65**, 033620 (2002); **65**, 053604 (2002).
[20] C. A. Müller and D. Delande, in *Les Houches 2009, Session XCI: Ultracold Gases and Quantum Information*, edited by C. Miniatura, L.-C. Kwek, M. Ducloy, B. Grémaud, B. G. Englert, L. F. Cugliandolo, and A. Ekert (Oxford University Press, Oxford, 2011).
[21] D. J. Thouless, J. Phys. C **6**, L49 (1973).
[22] R. C. Kuhn, O. Sigwarth, C. Miniatura, D. Delande, and C. A. Müller, New J. Phys. **9**, 161 (2007).
[23] L. Sanchez-Palencia, D. Clément, P. Lugan, P. Bouyer, and A. Aspect, New J. Phys. **10**, 045019 (2008).
[24] B. Kramer and A. MacKinnon, Rep. Prog. Phys. **56**, 1469 (1993).

[25] D. J. Atkins, H. M. Wiseman, and P. Warszawski, Phys. Rev. A **67**, 023802 (2003).

[26] W. K. Hensinger, A. G. Truscott, B. Upcroft, M. Hug, H. M. Wiseman, N. R. Heckenberg, and H. Rubinsztein-Dunlop, Phys. Rev. A **64**, 033407 (2001).

[27] M. Holland, S. Marktsteiner, P. Marte, and P. Zoller, Phys. Rev. Lett. **76**, 3683 (1996).

[28] E. Joos, H. D. Zeh, C. Kiefer, D. Giulini, J. Kupsch, and I.-O. Stamatescu, *Decoherence and the Appearence of a Classical World in Quantum Theory* (Springer, Berlin, 2003).

[29] C. Miniatura, R. C. Kuhn, D. Delande, and C. A. Müller, Eur. Phys. J. B **68**, 353 (2009).

[30] S. A. Gurvitz, Phys. Rev. Lett. **85**, 812 (2000).